

# Assessment of biological characteristics of adipose tissue-derived stem cells co-labeled with Molday ION Rhodamine B<sup>TM</sup> and green fluorescent protein *in vitro*

HUA NAN<sup>1</sup>, JIACHENG HUANG<sup>1</sup>, HONGMIAN LI<sup>2</sup>, QIONG LI<sup>1</sup> and DALIE LIU<sup>1</sup>

<sup>1</sup>Plastic Surgery Institute, Zhujiang Hospital, Southern Medical University, Guangzhou, Guangdong 510282;

<sup>2</sup>Plastic Surgery Institute, Zhongshan Hospital, Sun Yat-Sen University, Guangzhou, Guangdong 510275, P.R. China

Received March 13, 2013; Accepted August 30, 2013

DOI: 10.3892/mmr.2013.1694

**Abstract.** The current study aimed to investigate adipose tissue-derived stem cells (ADSCs) *in vivo* by multimodality imaging following implantation for cellular therapy. The biological characteristics of ADSCs co-labeled with Molday ION Rhodamine B<sup>TM</sup> (MIRB) and green fluorescent protein (GFP) were studied *in vitro*. Following rat ADSC isolation and culture, a combined labeling strategy for ADSCs based on genetic modification of the reporter gene GFP with lentiviral vector expression enhancement and physical MIRB labeling was performed. Cell viability, proliferation, membrane-bound antigens and multiple differentiation ability were compared between the labeled and unlabeled ADSCs. The ADSCs were successfully labeled with GFP and MIRB, showing various fluorescent colors for marker identification. The fluorescence emitted by the GFP protein was sustained and exhibited stable expression, while MIRB fluorescence decreased with time. Compared with the unlabeled ADSCs, no significant differences were detected in cell viability, proliferation, membrane-bound antigens and multiple differentiation ability in the co-labeled samples ( $P>0.05$ ). No significant effects on the biophysical properties of ADSCs were observed following co-labeling with lentiviral vectors encoding the gene for emerald green fluorescent protein and MIRB. The ADSCs were able to be efficiently tracked *in vitro* and *in vivo* by multimodality imaging thus, the co-labeling approach provides a novel strategy for therapeutic gene studies.

## Introduction

As an abundant and readily accessible source of multipotent stem cells, adipose tissue-derived stem cells (ADSCs) have

been extensively investigated for their specific therapeutic properties and are considered to be an ethical, practical and biologically appropriate cell population for cell therapy (1). An important approach leading to successful stem cell therapy is cell tracking *in vivo*, where a nontoxic, biocompatible, efficient and highly sensitive exogenous cell marker is required.

Green fluorescent protein (GFP) is capable of exhibiting fluorescence in living cells and has been widely used as a lineage marker for mammalian cells, predominantly as a pathological tracer following sacrifice of the animal and subsequent animal tissue slice culture (2). Although the fluorescent signal emitted from GFP may be easily detected with optical imaging, fluorescence microscopy or flow cytometry, there remains certain disadvantages in the practical application of these techniques. Magnetic resonance imaging (MRI), which may be used to track transplanted stem cells labeled with superparamagnetic ironoxide (SPIO), possesses the ability to non-invasively track and allow real-time imaging of injected labeled cells (3). Therefore, the introduction of SPIO into ADSCs labeled with lentiviral vectors encoding the gene for emerald green fluorescent protein (lenti-eGFP) is hypothesized to result in a non-pathological tracer *in vivo*, which may be observed by MRI. However, results showed that no biological characteristics of transplanted cells were detected by MRI and no regenerative and differentiated cells from exogenous and endogenous transplanted cells were distinguished.

In the current study, we propose that co-labeling cells with eGFP and SPIO may play a synergetic role in cell labeling. Whether this approach results in adverse effects on the biophysical properties of cells remains unknown, thus further investigations are required.

Molday ION Rhodamine B<sup>TM</sup> (MIRB) is an iron oxide-based superparamagnetic contrast reagent of a colloidal size of 50 nm. The colloidal particle may be visualized by MRI and fluorescence due to the labeling of rhodamine B (4). The excitation and emission wavelengths of this fluorescent dye are 555 and 565-620 nm, respectively. In the present study, based on genetic modification with the reporter genes eGFP by lenti-eGFP and physical labeling with MIRB, a combined labeling strategy for ADSCs was established. The feasibility of rat ADSCs co-labeled with lenti-eGFP and MIRB and the

---

Correspondence to: Dr Dalie Liu, Plastic Surgery Institute, Zhujiang Hospital, Southern Medical University, 253 Gongye Road, Guangzhou, Guangdong 510282, P.R. China  
E-mail: dl\_liu2013@126.com

**Key words:** adipose tissue-derived stem cells, Molday ION Rhodamine B<sup>TM</sup>, green fluorescent protein, cell labeling, *in vitro*

biological characteristics of these labeled ADSCs were also investigated.

## Materials and methods

**Preparation and characterization of ADSCs.** ADSCs were prepared following a method described by Zuk *et al.* (5) with modifications. Subcutaneous adipose tissue (3–4 g) was obtained from the abdominal and inguinal regions of adult male Sprague-Dawley rats (~200 g each). Following removal of debris and blood cells by washing with phosphate-buffered saline (PBS), the excised adipose tissue was minced and digested with 2 mg/ml collagenase I (Sigma-Aldrich, St. Louis, MO, USA) at 37°C for 30 min. Collagenase activity was neutralized by the addition of Dulbecco's modified Eagle's medium with Ham's F12 nutrient mixture (Gibco, Carlsbad, CA, USA) containing 15% fetal bovine serum (FBS; Thermo Fisher Scientific Inc., Rockford, IL, USA). The digested adipose tissue was filtered with a 100- $\mu$ m nylon membrane to eliminate the undigested fragments. Following centrifugation at 1,000  $\times$  g for 5 min (X-12R Benchtop Centrifuge; Beckman Coulter, Miami, FL, USA), cell pellets were resuspended in cell-culture medium (CCM) and cultivated at 37°C in 5% CO<sub>2</sub> for 24 h. Following removal of unattached cells and debris, fresh CCM containing 15% FBS was added and the adherent cells were cultured at 37°C in 5% CO<sub>2</sub>. The medium was changed following two days of incubation and every two days thereafter. Once attached cells reached 80–90% confluency and cultures were trypsinized and passaged at a ratio of 1:2. ADSCs from the third passage expansion were washed with PBS and detached from the culture dish using 0.25% trypsin-ethylenediamine tetra-acetic acid (Gibco). Cells were incubated with phycoerythrin-conjugated anti-mouse antibodies against CD34, CD44, CD45 and CD105 (eBioscience, San Diego, CA, USA) for 30 min at 4°C in the dark. Isotype antibodies served as a control. Cells were washed with PBS and analyzed by flow cytometry (Beckman Coulter Inc., Brea, CA, USA). Animal care and procedures were approved by the Animal Care and Use Committee of Southern Medical University (Guangzhou, China) and all experiments were conducted in accordance with the institutional guidelines.

**ADSC transduction and examination of GFP fluorescence.** Lenti-eGFP were produced with Lipofectamine 2000 (Invitrogen Life Technologies, Carlsbad, CA, USA) by cotransfection of 293FT cells and expression of a packaging plasmid. Lenti-eGFP viruses were transfected into 293T cells with Lipofectamine 2000 (Invitrogen Life Technologies) and then produced in 293T cells. Infection was performed at 37°C and 5% CO<sub>2</sub> for 2 h. At 72 h after infection, cells were observed under a fluorescence microscope (TE2000; Nikon, Tokyo, Japan) and five representative high power fields were selected to analyze the fluorescence intensities of GFP-positive cells. Infection efficiency of eGFP expressed in ADSCs one week following transduction was examined using the fluorescence-activated cell sorting (FACS) technique.

**Cell labeling with MIRB.** Medium (1 ml) containing passage 3 (P3) rat ADSCs was plated in a 6-well plate (1 $\times$ 10<sup>4</sup> cells/cm<sup>2</sup>) and incubated at 37°C with 5% CO<sub>2</sub> overnight. The MIRB

reagent (BioPAL, Inc., Worcester, MA, USA) containing 2 mg/ml Fe<sup>3+</sup> was added, resulting in a final Fe<sup>3+</sup> concentration of 10  $\mu$ g/ml. Following overnight incubation, the MIRB-containing medium was removed by aspiration and ADSCs were washed three times with PBS to remove extracellular MIRB. MIRB-labeled ADSCs were incubated at 37°C with 5% CO<sub>2</sub> in CCM for subsequent experiments.

**Cellular staining for intracellular iron.** Cell profiles and intracellular iron particles were identified using prussian blue staining. Cells were continuously incubated for 15 min with 2% potassium ferrocyanide in 6% hydrochloric acid and counterstained with nuclear fast red for 3 min. Labeling efficiency was analyzed by light microscopy (Olympus CK2; Olympus Optical Co. Ltd., Tokyo, Japan) and cells exhibiting blue intracellular particles were considered to be prussian blue-positive.

The distribution of the SPIO particles within the cells was examined under transmission electron microscopy (TEM; JEM1400; Jeol Ltd., Tokyo, Japan). Harvested labeled ADSCs were immersed in 2.5% buffered glutaraldehyde at 4°C for 1 h and fixed with 1% osmium tetroxide (Fluka, Sigma-Aldrich) for 2 h for observation.

**Groups.** ADSCs were divided into four groups according to the labeling treatment: Group 1, labeled with lenti-eGFP; group 2, labeled with MIRB; group 3, labeled with lenti-eGFP and MIRB; and group 4, control, with no labeling. ADSCs in the four groups were incubated under the same conditions for further assessment.

**Measurement of ADSC viability.** Cell proliferation in the labeled and unlabeled groups was monitored using a Trypan blue exclusion assay (Trypan Blue Staining Cell Viability Assay Kit, Shanghai Biyuntian Biological Co., Shanghai, China). The cell suspension (5  $\mu$ l) was mixed with 5  $\mu$ l 0.4% Trypan blue solution for 1 min and 100 cells were quantified using a hemocytometer (Neubauer cell counting chamber, DRM-700, CELL-VU CBC; Millenium Sciences, Inc., New York, NY, USA) for each assay. Cell viability was evaluated by the Trypan blue exclusion rate calculation (unstained cells / total number of cells  $\times$  100).

**Flow cytometric analysis of apoptosis.** Apoptosis was evaluated by FACS analysis using the Annexin V/PE Apoptosis Detection kit I (BD Biosciences, San Jose, CA, USA). The lenti-eGFP and MIRB co-labeled ADSCs on 12 well-plates were harvested by trypsinization after 1, 2, 3 and 4 weeks, respectively. Following FBS containing culture media neutralization and PBS washing, cells were resuspended in 100  $\mu$ l Annexin V binding buffer, and stained in the dark with 4  $\mu$ l Annexin V/PE (marker for apoptosis) and 4  $\mu$ l 7-AAD (a necrosis marker) for 15 min at room temperature. Following the addition of 400  $\mu$ l Annexin V binding buffer, 10,000 cells/sample were measured using a FACSCalibur flow-cytometer with CellQuest software (Becton-Dickinson, Franklin Lakes, NJ, USA).

**Induction of adipogenic and osteogenic differentiation of ADSCs.** Following the aforementioned pretreatment, the

Table I. Induction media.

Induction type	Induction component	Induction period (days)
Adipogenic	DMEM	12
	Streptomycin (5 $\mu$ g/ml)	
	Penicillin (5 U/ml)	
	FBS (5%)	
	Biotin (33 mM)	
	Pantothenate (17 mM)	
	Bovine insulin (10 $\mu$ M)	
	Isobutyl-methylxanthine (250 $\mu$ M)	
	Indomethacin (200 $\mu$ M)	
	Dexamethasone (1 $\mu$ M)induction	
Osteogenic	DMEM	28
	Streptomycin (5 $\mu$ g/ml)	
	Penicillin (5 U/ml)	
	FBS (10%)	
	$\beta$ -glycerophosphate (10 mM)	
	Ascorbate-2-phosphate (50 $\mu$ M)	
	1,25-(OH) <sub>2</sub> vitamin D <sub>3</sub> (10 nM)	

DMEM, Dulbecco's modified Eagle's medium; FBS, fetal bovine serum.

co-labeled ADSCs were induced by adipogenic and osteogenic induction (Table I). For adipocytic induction, the co-labeled ADSCs were cultured in DMEM supplemented with 5  $\mu$ g/ml streptomycin, 5 U/ml penicillin, 5% FBS, 1  $\mu$ M dexamethasone (Sigma-Aldrich), 250  $\mu$ M isobutyl-methylxanthine (Sigma-Aldrich), 10  $\mu$ M bovine insulin (Sigma-Aldrich), 17 mM pantothenate (Sigma-Aldrich), 200  $\mu$ M indometacin (Sigma-Aldrich) and 33 mM biotin (Sigma-Aldrich). After 12 days of induction at 37°C in 5% CO<sub>2</sub>, cells were stained with Oil Red O (Sigma-Aldrich). For osteogenic induction, the cells were cultured in DMEM supplemented with 5  $\mu$ g/ml streptomycin, 5 U/ml penicillin, 10% FBS, 10 nM 1,25-(OH)<sub>2</sub> vitamin D<sub>3</sub>, 50  $\mu$ M of ascorbate-2-phosphate (Biojet, Guangzhou, China) and 10 mM  $\beta$ -glycerolphosphate (Sigma-Aldrich). After 28 days of induction at 37°C in 5% CO<sub>2</sub>, staining was performed with Alizarin Red (Sigma-Aldrich).

**Transdifferentiation potential of co-labeled ADSCs.** Adipogenic differentiation was evaluated by staining cytoplasmic lipid deposits in the co-labeled ADSCs. Cells were plated at 2.5x10<sup>4</sup> cells/cm<sup>2</sup> and allowed to reach 90% confluency, followed by incubation for three cycles in induction/maintenance medium. ADSCs were cultured for seven days in an adipogenic maintenance medium. Cells were fixed with 10% buffered formalin and stained with Oil red O.

Osteogenic transdifferentiation was evaluated by Alizarin red staining of the induced co-labeled ADSCs. Cells were plated at 4.2x10<sup>3</sup> cells/cm<sup>2</sup> and incubated for 24 h in CCM. Following incubation, cells were transferred to osteogenic

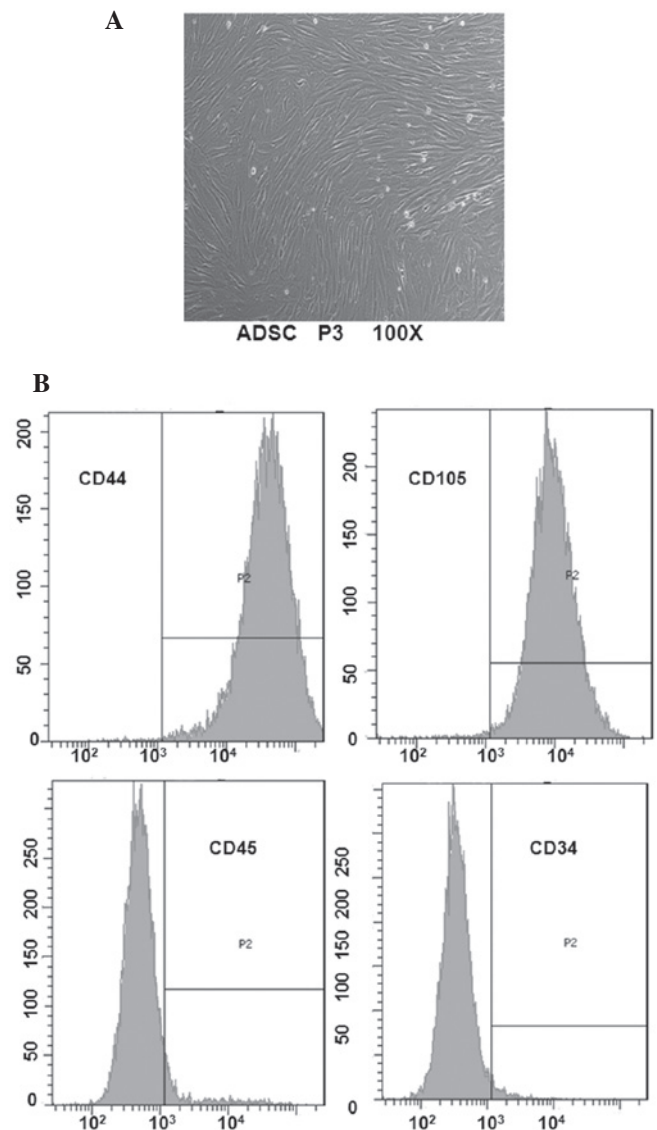


Figure 1. Characterization of human ADSCs. (A) Fibroblast-like rat ADSCs P3 with slim bodies (magnification, x100). (B) ADSCs positive for P3 homogeneous markers of the surface proteins, CD44 and CD105, and negative for the hematopoietic lineage markers of CD45 and CD34. ADSCs, adipose tissue-derived stem cells; P3, passage 3.

induction medium and cultured for 21 days and the medium was changed every 3 days. Cells were fixed and stained with Alizarin red staining to assess mineralization.

**Statistical analysis.** SPSS statistical package, version 11.0 (SPSS Inc., Chicago, IL, USA) was used for Student's unpaired t-test statistical analysis. Data are expressed as the mean  $\pm$  SD. The Kruskal-Wallis rank sum test was used to determine the difference in absorbance of MTT for the comparison of labeled and unlabeled ADSCs. P<0.05 was considered to indicate a statistically significant difference.

## Results

**ADSC morphology and expression of surface antigens.** To determine ADSC features, morphological observation and surface antigen identification was performed by flow

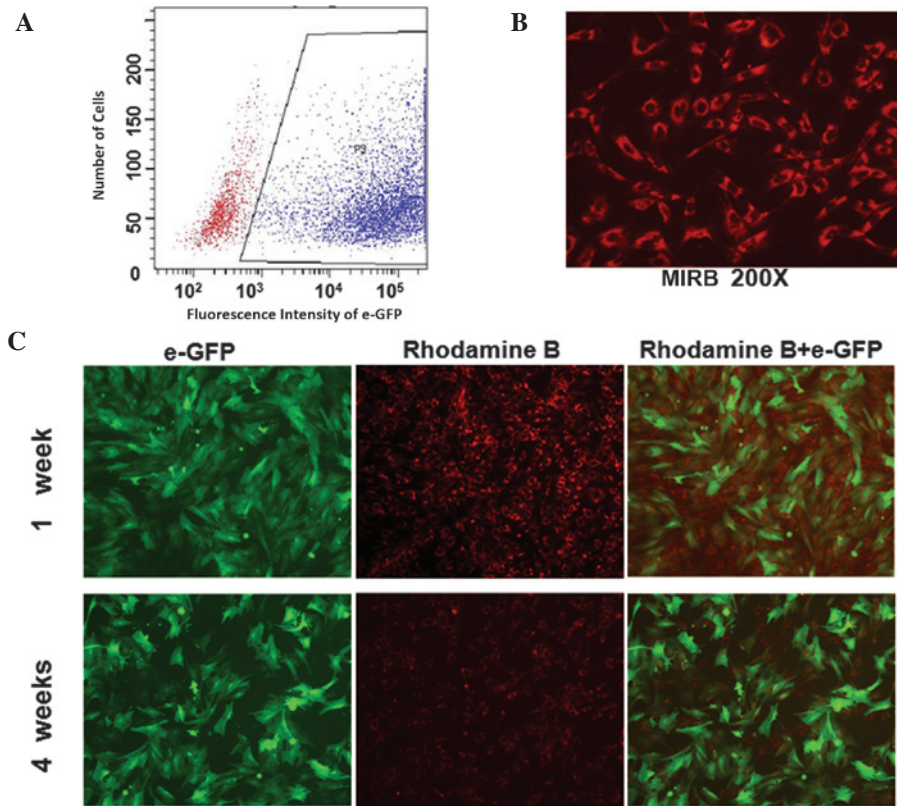


Figure 2. Labeling efficiency and fluorescence intensity of co-labeled human ADSCs. (A) With a multiplicity of infection of 400:1, >81.4% of ADSCs were infected with GFP on day five demonstrated by flow cytometry. (B) Red fluorescence emitted by MIRB-labeled ADSCs (magnification, x200). (C) Strong and uniform fluorescence intensity for GFP expression on the surface of co-labeled ADSCs, the decrease of the rhodamine B signal for MIRB expression following culturing the co-labeled ADSCs for four weeks *in vitro* and the combined signal for GFP and MIRB (magnification, x100). The corresponding fluorescence intensities for one week are shown. ADSCs, adipose tissue-derived stem cells; MIRB, Molday Ion Rhodamine B™; GFP, green fluorescent protein; Spio, superparaagnetic iron oxide.

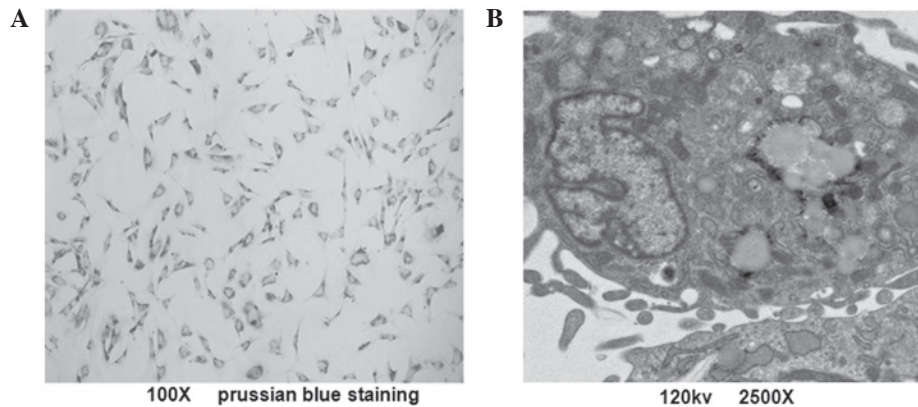


Figure 3. Intracellular iron particle distribution. (A) Labeling rate of human ADSCs was ~100% observed by prussian blue staining and light microscopy (magnification, x100). (B) Superparaagnetic iron oxide particles were located in the endosomal vesicles of labeled ADSCs (magnification, x1500; 150 kv). ADSCs, adipose tissue-derived stem cells.

cytometry. Following primary culture, a small population of single spindle-shaped cells was presented with adherent ADSCs. On days 5-7, following initial plating, the cells began to form colonies and became confluent (Fig. 1A). When ADSCs were passaged to P3, the purified ADSCs retained the morphology of uniform fibroblast-like cells. Cell surface phenotype analysis indicated that the ADSC population was positive for CD44 and CD105, and negative for CD34 and CD45 (Fig. 1B).

*Labeling efficiency and fluorescence intensity of labeled ADSCs.* To characterize the co-labeled ADSCs, labeling efficiency was determined by flow cytometry and fluorescence intensity was examined via fluorescent and confocal microscopy (LSM 510 Confocal Laser Scanning Microscope, Carl Zeiss, Jena, Germany). With an MOI of 400:1, >81.4% of ADSCs infected with lenti-eGFP showed strong fluorescent signals for GFP expression on day 5 (Fig. 2A). Infected cells were labeled with 20 g/ml<sup>-1</sup> Fe<sup>3+</sup> MIRB and the percentage of

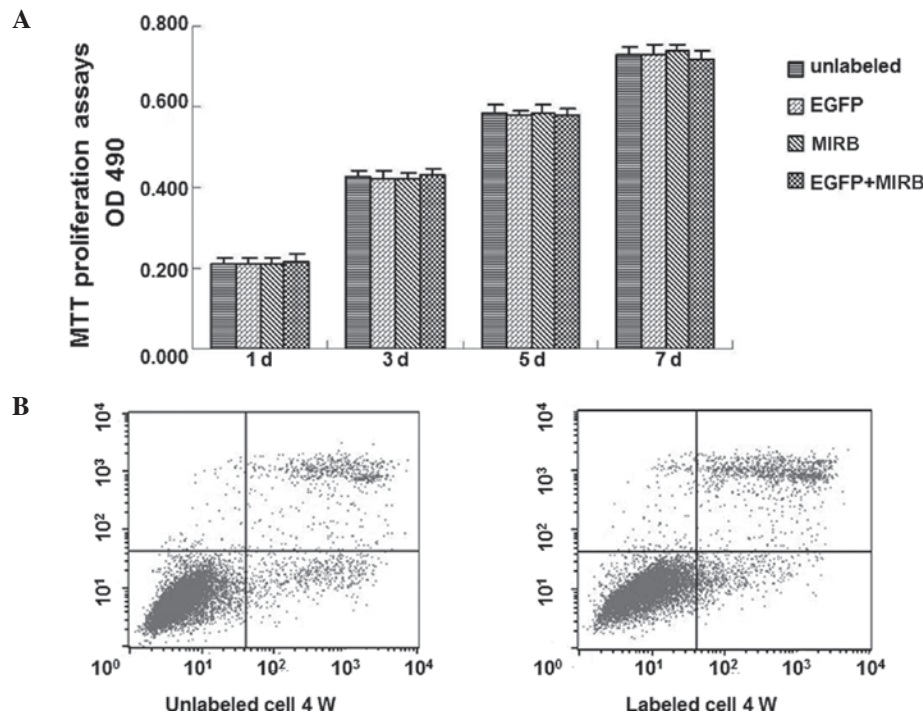


Figure 4. Viability, proliferation and apoptosis of the co-labeled human ADSCs. (A) MTT proliferation assays showed no marked differences among the four groups on day 1, 3, 5 and 7, respectively (determined at a wavelength of 490 nm). (B) Low rates of apoptosis and necrosis were observed in the co-labeled and unlabeled control groups following 4 weeks. ADSCs, adipose tissue-derived stem cells; SPIO, superparaagnetic iron oxide; EGFP, enhanced green fluorescent protein.

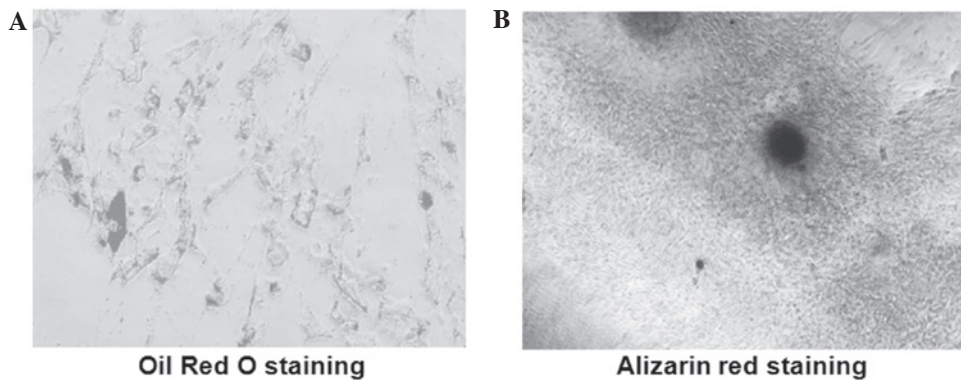


Figure 5. Transdifferentiation potential of co-labeled human ADSCs. (A) Oil Red O staining demonstrated the formation of lipid vacuoles occurred inside co-labeled cells. (B) Mineralization in the osteogenic differentiation was confirmed using Alizarin red staining. ADSCs, adipose tissue-derived stem cells.

rhodamine B-positive cells was >95% (Fig. 2B). Following culturing of the co-labeled ADSCs for four weeks *in vitro*, the green fluorescence expressed by eGFP remained stable while the red fluorescence expressed by MIRB was significantly decreased (Fig. 2C). These results indicate that ADSCs may be labeled with GFP and MIRB successfully and identified via specific colored fluorescence. The fluorescence emitted by GFP was sustained and stably expressed, while fluorescence with MIRB decreased with time.

**Intracellular iron particle distribution.** To determine the intracellular iron particle distribution of MIRB-labeled ADSCs, prussian blue staining was observed by light microscopy. The labeling rate of ADSCs was ~100%, according to the observation of blue-stained iron particles (Fig. 3A). A similar

proportion was observed with rhodamine B staining. TEM results revealed that the SPIO particles were located in the endosomal vesicles of labeled ADSCs (Fig. 3B). These results indicate that SPIO and rhodamine B were coupled together in MIRB and their expression tended to be synchronized.

**Lenti-eGFP and MIRB effect on the viability, proliferation and apoptosis of ADSCs.** To investigate the effect of the markers on the proliferation and the toxicity of markers to ADSCs, cell viability and proliferation were determined by the trypan blue exclusion test and MTT assay, while the cell apoptosis was observed by flow cytometry. Trypan blue exclusion testing showed a mean cell viability of  $98.12 \pm 1.26\%$  for the GFP-labeled ADSCs and  $98.72 \pm 1.65\%$  for the MIRB-labeled ADSCs, respectively. The mean viability of the unlabeled

ADSCs was  $98.63 \pm 1.41\%$  and  $99.06 \pm 1.08\%$ , respectively. However, no significant differences on the exclusion rate were identified between labeled and unlabeled cells ( $P > 0.05$ ) at all time points. MTT proliferation assays showed no marked differences among the four groups on day 1, 3, 5 and 7, respectively (Fig. 4A). Low rates of apoptosis and necrosis in co-labeled and control groups were observed following 1, 2, 3 and 4 weeks, respectively (Fig. 4B). These results indicate that co-labeling of ADSCs with lenti-eGFP and MIRB is applicable and exhibited no significant adverse effect on ADSC viability, proliferation and apoptosis.

**Transdifferentiation potential of co-labeled ADSCs.** To assess the effect of co-labeling on ADSCs trans-differentiation potency, the multipotency of labeled and unlabeled ADSCs was detected with osteogenic and adipogenic induction, respectively. In adipogenic differentiation, Oil Red O staining demonstrated that the formation of lipid vacuoles occurred inside co-labeled cells (Fig. 5A) and the mineralization in the osteogenic differentiation was confirmed using alizarin red staining (Fig. 5B). These results indicate that ADSCs labeled with lenti-eGFP and MIRB have the stem cell potential for multi-directional differentiation.

## Discussion

The monitoring of the migration and homing of transplanted cells, as well as the engraftment efficiency and functional capability *in vivo* has become a critical issue with the rise of stem cell-based therapies. Stem cells have therapeutic effects in refractory diseases (6,7). However, the mechanisms underlying cell therapy remain unclear and their actions *in vivo* require further investigation. Thus, the approach of transplanted stem cell imaging has become a focus of stem cell studies and is widely accepted as a preclinical tool to evaluate novel therapeutic strategies. At present, to improve the monitoring of cellular dynamics of the transplanted stem cells *in vivo*, a reliable technique for tracking grafted stem cells is required.

A model cell tracer requires the following features: i) a sufficiently high signal for detection, ii) is not eluted, iii) is not metabolized and iv) is specific to labeled cells. As a labeling protein technology, GFP gene-tagging is most extensively applied due to its high efficiency, non-toxicity, stabilization and capability for long-term follow-up testing (8,9). Although GFP is frequently used as an animal pathological tracer, disadvantages are occasionally encountered in the practical application as fluorescent labeling technology is difficult to assess by dynamic and noninvasive monitoring. Previously, it has been shown that MRI is effective in tracking the distribution of transplanted stem cells *in vivo* by labeling with SPIO particles. SPIO effectively labels numerous cell types and the labeled cells are able to be monitored for a number of weeks (10,11). However, the technology also has disadvantages of short tracer time and low spatial resolution. Moreover, cell death is observed in a significant number of SPIO-labeled stem cells shortly following transplantation due to the resulting proapoptotic and cytotoxic microenvironment (12). The SPIO nanoparticles were observed to remain in the interstitial compartment for a period of time or were taken up by macrophages and were not distinguished by prussian blue staining.

Therefore, the signal voids observed from MRI may not necessarily represent living stem cells (13). Normal cellular uptake mechanisms are inadequate in loading cells with a tracking label long-term, but the multimodality imaging of cell tracking techniques permits analysis of transplantation efficiency and the potential migration, distribution and turnover of transplanted cells *in vivo*.

ADSCs have similar surface markers and gene profiling to bone marrow stem cells and are readily available with clonogenic potency and a robust proliferative capacity (14,15). The aforementioned advantages have resulted in this population becoming a predominant candidate for cell therapy and selection for the current study. As previously demonstrated, SPIO showed no effect on ADSC viability, transdifferentiation potential or cell-factor secretion (16), while MIRB was observed to exhibit a high physical labeling efficiency without any transfection agent and was less toxic (17). Therefore, a novel SPIO contrast agent, MIRB, which may be visualized by MRI and fluorescence microscopy was used in the current study. To obtain an accurate assessment of the migration and turnover of the transplanted ADSCs *in vivo*, the detection, tracking and multimodal image acquisition were conducted for a number of months. In the present study, a co-labeled method was used, with lenti-eGFP infection of P3 ADSCs followed by a direct transfection of the GFP-ADSCs with MIRB.

Present results showed that the GFP protein was steadily expressed with the GFP-labeled cell proliferation. A CCK-8 assay was used to determine cell viability and flow cytometric analysis of cell apoptosis and cycles suggested that co-labeling of lenti-eGFP and MIRB was noncytotoxic, indicating its potential use in cell therapy. The multipotency of labeled and unlabeled ADSCs was confirmed by osteogenic and adipogenic induction with specific differentiation media. Osteogenic and adipogenic differentiation assessments showed that no significant difference occurred in cell viability, proliferation and multiple differentiation capability between the labeled and unlabeled ADSCs, demonstrating that lenti-eGFP and MIRB did not affect ADSC viability, which is similar to the results of a previous study concerning SPIO (18).

After four weeks, a marginal decrease of MIRB red fluorescence intensity was identified in the co-labeled ADSCs; however, the GFP green fluorescence was observed to be sustained. The differences in stability demonstrated that MIRB allows the observation of grafted cell migration and distribution for a short-time period only, while GFP allows a longer period of observation. Due to the biological degradation of MIRB, the number of surviving labeled cells *in vivo* may be underestimated by MRI. Considering the drawbacks of label leakage and false positive signals with macrophage engulfed debris in this direct cell labeling (19,20), SPIO is therefore, inappropriate for use in long-term observation *in vivo*. By contrast, GFP may verify the presence of living stem cells at target sites and may eliminate adverse factors, including hemorrhage and cell death (21) and its application for implanted cell monitoring *in vivo* remains an option. Moreover, co-labeling of lenti-eGFP and MIRB may be improved by obtaining cell migration data via noninvasive methods, including MRI in early stages combined with a pathological tracer technique-like labeling immunofluorescent

staining and laser scanning confocal microscopy methods in later stages.

In conclusion, the biological characteristics of ADSCs labeled with MIRB and GFP did not exhibit any significant differences in cell viability, proliferation, membrane-bound antigens and multiple differentiation ability compared with unlabeled ADSCs *in vitro* and the co-labeling technique may be employed for cell observation under a number of conditions, without any significant adverse effects. Real-time tracking for transplanted cells by MRI and pathological tracer techniques using immunofluorescent staining and laser scanning confocal microscopy may aid in understanding the mechanism of stem cell transplantation therapy. Dynamic tracking MRI results require further investigation via GFP expressed green fluorescence. The technology developed in the current study improves the accuracy for observation of the existence and functional status of transplanted cells *in vivo* and provides a novel approach for curative cell therapy evaluation.

### Acknowledgements

This study was supported by a grant from the National Natural Science Foundation of China (grant no. 81171831).

### References

- De Ugarte DA, Morizono K, Elbarbary A, *et al*: Comparison of multi-lineage cells from human adipose tissue and bone marrow. *Cells Tissues Organs* 174: 101-109, 2003.
- Bauer G, Dao MA, Case SS, *et al*: In vivo biosafety model to assess the risk of adverse events from retroviral and lentiviral vectors. *Mol Ther* 16: 1308-1315, 2008.
- Bulte JW and Kraitchman DL: Iron oxide MR contrast agents for molecular and cellular imaging. *NMR Biomed* 17: 484-499, 2004.
- Addicott B, Willman M, Rodriguez J, Padgett K, Han D, Berman D, Hare JM and Kenyon NS: Mesenchymal stem cell labeling and in vitro MR characterization at 1.5T of new SPIO contrast agent: Molday ION Rhodamine-B™. *Contrast Media Mol Imaging* 6: 7-18, 2011.
- Zuk PA, Zhu M, Mizuno H, Huang J, Futrell JW, Katz AJ, Benhaim P, Lorenz HP and Hedrick MH: Multilineage cells from human adipose tissue: implications for cell-based therapies. *Tissue Eng* 7: 211-228, 2001.
- Caplan AI: Review: mesenchymal stem cells: cell-based reconstructive therapy in orthopedics (Review). *Tissue Eng* 11: 1198-1211, 2005.
- Dyson SC and Barker RA: Cell-based therapies for Parkinson's disease. *Expert Rev Neurother* 11: 831-844, 2011.
- Ward TH and Lippincott-Schwartz J: The uses of green fluorescent protein in mammalian cells. *Methods Biochem Anal* 47: 305-337, 2006.
- Serganova I, Mayer-Kukuck P, Huang R and Blasberg R: Molecular imaging: reporter gene imaging. *Handb Exp Pharmacol* 185: 167-223, 2008.
- Zhu XM, Wang YX, Leung KC, Lee SF, Zhao F, Wang DW, Lai JM, Wan C, Cheng CH and Ahuja AT: Enhanced cellular uptake of aminosilane-coated superparamagnetic iron oxide nanoparticles in mammalian cell lines. *Int J Nanomedicine* 7: 953-964, 2012.
- Lee ES, Chan J, Shuter B, *et al*: Microgel iron oxide nanoparticles for tracking human fetal mesenchymal stem cells through magnetic resonance imaging. *Stem Cells* 27: 1921-1931, 2009.
- Domen J and Weissman IL: Self-renewal, differentiation or death: regulation and manipulation of hematopoietic stem cell fate. *Mol Med Today* 5: 201-208, 1999.
- Kraitchman DL, Heldman AW, Atalar E, Amado LC, Martin BJ, Pittenger MF, Hare JM and Bulte JW: In vivo magnetic resonance imaging of mesenchymal stem cells in myocardial infarction. *Circulation* 107: 2290-2293, 2003.
- Zhu Y, Liu T, Song K, Fan X, Ma X and Cui Z: Adipose-derived stem cell: a better stem cell than BMSC. *Cell Biochem Funct* 26: 664-675, 2008.
- Taléns-Visconti R, Bonora A, Jover R, Mirabet V, Carbonell F, Castell JV and Gómez-Lechón MJ: Hepatogenic differentiation of human mesenchymal stem cells from adipose tissue in comparison with bone marrow mesenchymal stem cells. *World J Gastroenterol* 12: 5834-5845, 2006.
- Wang L, Deng J, Wang J, *et al*: Superparamagnetic iron oxide does not affect the viability and function of adipose-derived stem cells, and superparamagnetic iron oxide-enhanced magnetic resonance imaging identifies viable cells. *Magn Reson Imaging* 27: 108-119, 2009.
- Ren Z, Wang J, Zou C, Guan Y and Zhang YA: Labeling of cynomolgus monkey bone marrow-derived mesenchymal stem cells for cell tracking by multimodality imaging. *Sci China Life Sci* 54: 981-987, 2011.
- Arbab AS, Yocum GT, Rad AM, Khakoo AY, Fellowes V, Read EJ and Frank JA: Labeling of cells with ferumoxides-protamine sulfate complexes does not inhibit function or differentiation capacity of hematopoietic or mesenchymal stem cells. *NMR Biomed* 18: 553-559, 2005.
- Acton PD and Zhou R: Imaging reporter genes for cell tracking with PET and SPECT. *Q J Nucl Med Mol Imaging* 49: 349-360, 2005.
- Higuchi T, Anton M, Dumler K, *et al*: Combined reporter gene PET and iron oxide MRI for monitoring survival and localization of transplanted cells in the rat heart. *J Nucl Med* 50: 1088-1094, 2009.
- Qiu B, Treuting P, Zhan X, Xie D, Frevert CW and Yang X: Dual transfer of GFP gene and MGd into stem-progenitor cells: toward in vivo MRI of stem cell-mediated gene therapy of atherosclerosis. *Acad Radiol* 17: 547-552, 2010.